

Ultrafast Hot-Carrier Dynamics at Chemically Modified Ge Interfaces Probed by SHG

Arthur McClelland, Vasiliy Fomenko, and Eric Borguet

J. Phys. Chem. B, **2006**, 110 (40), 19784-19787 • DOI: 10.1021/jp0460700 • Publication Date (Web): 06 September 2006

Downloaded from <http://pubs.acs.org> on March 16, 2009

More About This Article

Additional resources and features associated with this article are available within the HTML version:

- Supporting Information
- Access to high resolution figures
- Links to articles and content related to this article
- Copyright permission to reproduce figures and/or text from this article

[View the Full Text HTML](#)



ACS Publications
High quality. High impact.

Ultrafast Hot-Carrier Dynamics at Chemically Modified Ge Interfaces Probed by SHG[†]

Arthur McClelland, Vasily Fomenko, and Eric Borguet*

Department of Chemistry, Temple University, Philadelphia, Pennsylvania 19122

Received: August 31, 2004; In Final Form: March 17, 2005

Time-resolved second-harmonic generation (SHG) was used to study the hot-carrier dynamics and nonlinear optical properties of S-terminated and Cl-terminated Ge(111) interfaces on the femtosecond time scale. The hot-carrier second-order nonlinear optical susceptibilities were determined to be 720 ± 50 times greater than the valence-band second-order nonlinear optical susceptibilities for the Ge(111)–S system and 880 ± 100 times greater in the Ge(111)–Cl system. Furthermore, the ground- and excited-state second-order nonlinear optical susceptibilities are suggested to be out of phase for Ge(111)–S and Ge(111)–Cl systems, leading to a pump-induced decrease in the SHG signal as opposed to the increase in the SHG signal observed in the Ge(111)–GeO₂ system. Although the SHG response reaches a steady state in 415 ± 90 fs in the Ge(111)–GeO₂ system, a faster response is observed in the Ge(111)–S system, 220 ± 85 fs, and in the Ge(111)–Cl system, 172 ± 50 fs. This suggests significantly faster carrier cooling at the Ge(111)–Cl and Ge(111)–S interfaces, with significant implications for hot-carrier mediated device degradation, and migration to high-K dielectrics.

Introduction

How surface terminations affect semiconductor electrical properties is important in traditional semiconductor device engineering.¹ It is also relevant in the newer, related field of molecular electronics, which seeks to combine molecular chemistry and solid-state semiconductor technology with the objective of inducing novel and useful properties while maintaining semiconductor interfaces that are electrically passive and stable under ambient conditions.² This relevance explains in part the considerable interest in the wet chemical modification of semiconductors that draws extensively on well-established, solution-phase organosilane and organogermanium chemistry, spurred on by the success in wet-chemical H termination of Si.^{7–15}

Although the semiconductor industry is founded principally on silicon, there has been renewed interest in germanium because of the potential for faster devices resulting from the higher carrier mobility of Ge relative to Si.^{3,4} SiO₂, the native oxide of Si, is quite stable as a gate dielectric.^{5,6} The native oxide of germanium, GeO₂, however, is unstable and is in fact water soluble.⁵

A major question facing the design of these new Ge-based devices is how the various chemical terminations, required to provide a junction between molecules and the semiconductor, will affect device performance. A key issue is device degradation via hot-carrier thermalization.¹⁶

The experiments reported here addressed how hot-carrier dynamics are affected by different terminations of the Ge(111) interface on the femtosecond (10^{-15} s) time scale. Second-harmonic generation (SHG), known to be an excellent probe of buried interfaces, was used to investigate the ultrafast response with interface specificity.^{17,18}

Experimental Section

Ge–GeO₂ Sample Preparation. Ge wafers (undoped, Eagle Picher) were degreased by successive 10-min sonications in trichloroethylene (J. T. Baker, reagent grade), acetone (EM Science, reagent grade), and then methanol (Fisher Scientific, certified ACS grade). No additional treatment was performed on the oxidized samples before the experiments. All of the chemicals were used as received.

Preparation of GeS₂ Termination. The Ge sample was first degreased as described above, and then it was H terminated by dipping it in HF (48% Mallinckrodt, reagent grade) for 10 s and then ultrapure (> 18 M Ω .cm) water for 20 s, repeated five times. The H-terminated sample was then S terminated by placing it in (NH₄)₂S at 70 °C for 20 min.¹⁹ This passivating reaction is reported to be self limited to 2–3 monolayers.²⁰ The sulfide layer was determined to be ~ 1.8 -nm thick from ellipsometric measurements using interpolated optical constants: $n = 5.505$ and $k = 0.776$ for Ge²¹ and $n = 1.87$ for GeS₂ at 632.8 nm.²²

Preparation of Cl Termination. The clean, oxidized Ge samples were chloride terminated by dipping them in dilute (10%) HCl for 10 min.^{9,23} They were then rinsed briefly (< 5 s) in ultrapure water. The sample was finally blown dry with N₂. This procedure is reported to result in a monolayer of Cl-terminating Ge(111).^{9,23}

SHG Experimental Setup. The SHG experiments were performed with 800-nm, ~ 100 -fs, 76-MHz Ti:sapphire oscillator (Coherent Mira Seed) as described elsewhere.¹⁰ The p-polarized probe beam and the s-polarized pump beam pass, symmetrically off axis, through a 100-mm lens that focuses the beams to a 30 ± 4 - μ m circular spot size measured by the knife-edge technique. Typically, the s-polarized average pump power was 150 mW, which generates an excited carrier density of 1.8×10^{19} cm⁻³. A 50-mW p-polarized probe results in an excited carrier density of 9×10^{18} cm⁻³. The pump beam strikes the sample at an angle of 47°, and the probe beam strikes that sample at 43° forming ellipses on the surface. The elliptical shape of the

[†] Part of the special issue "Charles B. Harris Festschrift".

* To whom correspondence should be addressed. E-mail: eborguet@temple.edu.

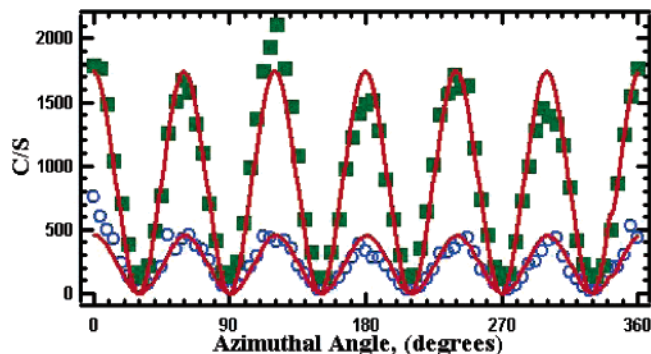


Figure 1. SHG-RA of Ge(111)–Cl p_{in}/s_{out} polarization combination (■) vs Ge(111)–GeO₂ (○).

focused beam as well as the different reflectivity of the p- (probe) and s- (pump) polarized beams were accounted for in calculating the density of the electron–hole pairs, N_{e-h} . Ge(111)–GeO₂ experiments were performed in laboratory ambient air at 295 K. The experiments on the Ge(111)–Cl and Ge(111)–S systems were carried out in a dry N₂ purge because of the instability of the terminations.⁹ SHG rotational anisotropy (SHG-RA) scans performed before and after the time-resolved SHG (TR-SHG) experiments showed unaltered SHG-RA patterns, thus ruling out the possibility of laser-induced changes of the interfaces under purge. The experiments done in the absence of a purge showed evidence of photo-oxidation of the GeS₂, as evidenced by SHG-RA patterns.⁹ This was presumably a result of the prolonged, intense illumination required for the TR-SHG experiments, significantly longer than that in the SHG-RA measurements and thus resulting in a greater cumulative photon flux.^{9,10} The pump beam delay was controlled by a stepper motor and a translation stage. Data were collected in 80-fs steps with a collection time of 1 s/data point. Multiple scans were averaged to achieve a better signal-to-noise ratio. The overlap of the pump and probe beams, as well as the divergence of the pump beam, was carefully controlled because these could lead to spurious dynamics.

Verification of S Termination. To verify that the surface had been properly chemically modified, the rotational anisotropy was taken in the purged environment before and after the S termination procedure. The changes in the SHG-RA signal are consistent with those reported previously.^{9,10}

Verification of Cl Termination. The p-in/s-out rotational anisotropy of Ge(111)–Cl typically has the same pattern, but a much higher signal level, than the Ge(111)–GeO₂ samples. The increase in signal level can be used as verification that the surface termination was altered.⁹ This difference could only be observed in the N₂ purge environment. If air was admitted to the sample, then the SHG-RA pattern rapidly evolved to that of the Ge(111)–GeO₂ samples. This rapid oxidation has been suggested by previous combined SHG and XPS experiments.⁹

Results and Discussion

The results of typical pump–probe SHG experiments from the different Ge interfaces are illustrated in Figure 2. For the Ge–S and Ge–Cl interfaces, a prompt dip in the SHG signal is observed around $t = 0$, (dotted lines in Figure 2), followed by an increase in signal at $t > 0$ to some final steady-state level. Although creation of excited electron–hole pairs in the Ge(111)–GeO₂ system results in an increase of the SHG on the picosecond time scale, a decrease of the SHG is observed for Ge(111)–Cl and Ge(111)–S. This is reminiscent of the difference observed between Si(111)–SiO₂ and Si(111)–H.²⁴

A linear, rather than quadratic, dependence of the bleach on excited carrier density was observed for Ge(111)–GeO₂ and Ge(111)–S (Figure 3). This behavior is consistent with a simple model where one assumes that the total second-order nonlinear susceptibility of the system, $\chi_s^{(2)}$, depends on the carrier density in the excited state and the ground state in the following manner

$$\chi_s^{(2)} = N\chi^{(2)} + N^*\chi^{*(2)} \quad (1)$$

where N^* and N are the photoexcited carrier (electron–hole pair) density and the valence-band electron density, respectively and $\chi^{*(2)}$ and $\chi^{(2)}$ are the nonlinear susceptibilities of the photoexcited carriers and valence-band, respectively.^{24,25} The linear term dominates the quadratic term in the bleach expression.^{1,25} The steady-state (i.e., at $\Delta t \gg 0$) $\chi^{*(2)}/\chi^{(2)}$ ratio in the Ge(111)–GeO₂ system was found to be 462 ± 20 using the initial excited carrier density for N^* and the valence electron density for N . However, at 3.5 ps, half the carriers excited by the pump were estimated to have diffused into the bulk, out of the region that was probed by SHG.²⁶ The $\chi^{*(2)}/\chi^{(2)}$ ratio was found to be 924 ± 40 for the Ge(111)–GeO₂ system, $-720 \pm$

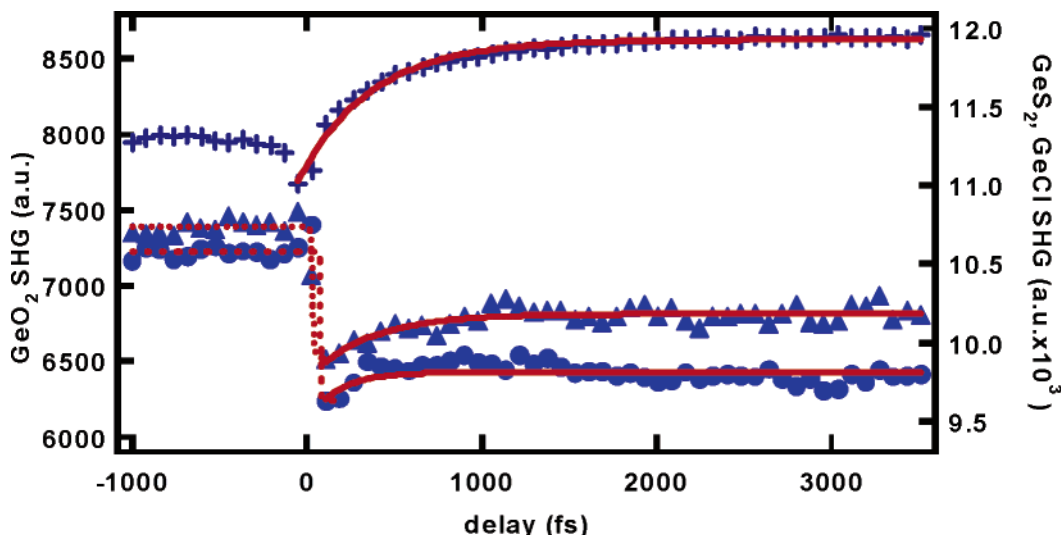


Figure 2. TD-SHG for Ge(111)–GeO₂, (+) Ge(111)–S (▲), and Ge(111)–Cl (●), performed at SHG-RA azimuth corresponding to a max of SHG-RA; s-pump (150–160 mW), p-probe (50 mW). N.B. The Ge(111)–S data is scaled (multiplied) by a factor of 4.7 on this graph to make the data presentation and comparison easier.

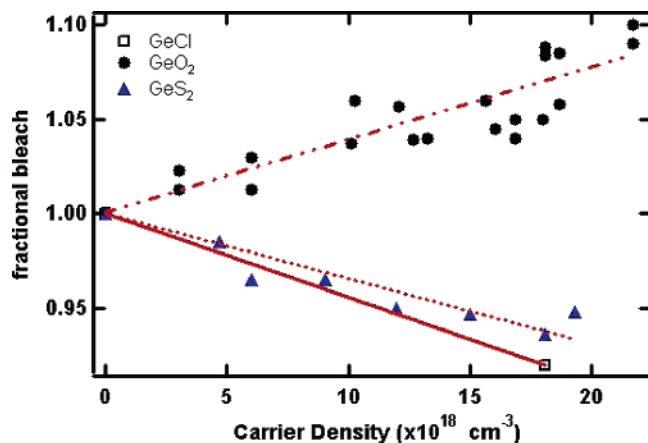


Figure 3. Fractional bleach at 2.5–3.5 ps vs carrier density; (●) GeO₂, (▲) GeS₂, (□) GeCl.

50 in the Ge(111)–S system, and -880 ± 100 in the Ge(111)–Cl system, taking into account the number of excited carriers present at 3.5 ps (i.e., the factor of 2 decrease in N^*).

The change in the linear optical response due to changes in the excited carrier density was calculated to be responsible for less than $1/10$ of the change in the SHG signal observed.²⁵ The change in the refractive index, due to the population of the excited carriers and to the laser-induced change in temperature, were also calculated and shown to be small.²⁵ The change in the TR-SHG response reflects the different nonlinear optical properties of the systems.

The most dramatic effect of the different surface terminations on the SHG response was the direction of the bleach. As previously reported²⁵ for Ge(111)–GeO₂, an increase in signal at positive times was observed but, surprisingly, the GeS and GeCl systems exhibited a decrease in signal at positive times, Figure 2. This can be explained by considering that the $\chi^{*(2)}$ is in phase with $\chi^{(2)}$ for the Ge(111)–GeO₂ system but out of phase for the Ge(111)–S and Ge(111)–Cl systems.

The time evolution of the SHG signal at $t > 0$ cannot be interpreted as resulting solely from the diffusion of carriers into the bulk and the corresponding change of N_{e-h} in eq 1.²⁵ In addition, a time evolution of $\chi^{*(2)}$ must also be considered. The time scale of this latter process was also found to depend on the chemical state of the interface. The trend seems to be the heavier the terminating surface atom (O vs Cl vs S) the quicker the SHG signal goes to a steady state. One possible explanation is that the surface deformation potential is changed by chemical termination in such a way as to accelerate the relaxation of hot carriers.²⁷ This, in turn, would affect the $\chi^{*(2)}$ of the system, leading to the more rapid initial change of the SHG signal (Figure 4).

The time evolution of $\chi^{*(2)}/\chi^{(2)}$ was extracted for the three different chemical terminations (Figure 4), as described previously.²⁵ The Ge(111)–GeO₂ system has a fast (~ 200 fs) and a slow (~ 4 ps) evolution. Only the slow component (> 2 ps) is resolved for the Ge(111)–S and Ge(111)–Cl systems. (See Table 2 for details.) The fast component, indicated by the prompt drop at $t = 0$, is too rapid to be resolved in these experiments. Nevertheless, the fast component appears to be a significant relaxation channel as the prompt initial response accounts for about $1/2$ of the change in $\chi^{*(2)}/\chi^{(2)}$.

The $\chi^{*(2)}(t)/\chi^{(2)}$ ratio was extracted from the data in Figure 2. In the Ge(111)–S and Ge(111)–Cl systems, the fast time constants appear to be too fast (< 80 fs) to be observed with the time resolution of our experiments.

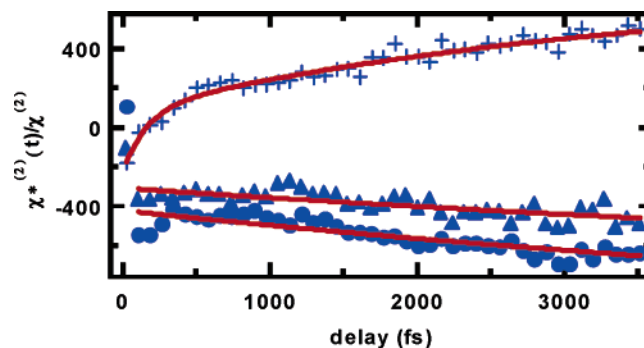


Figure 4. Evolution of $\chi^{*(2)}(t)/\chi^{(2)}$ ratio for Ge(111)–GeO₂, at an SHG-RA azimuth corresponding to a max of SHG-RA of p_{in}/p_{out} ; (+) GeO₂, (▲) GeS, (●) GeCl.

TABLE 1: SHG Steady-State Time Constants and Bleach for the Various Surface Terminations s-Pump (150–160 mW) p-Probe (50 mW) for the Data of Figure 2^a

	τ	bleach
Ge–GeO ₂	416 ± 17 fs	$8.4 \pm 0.4\%$
Ge–S	344 ± 80 fs	$-5.2 \pm 0.6\%$
Ge–Cl	172 ± 50 fs	$-7.6 \pm 0.5\%$

^a The bleach is defined as $(I_{sat} - I_{ini})/I_{ini}$, where I_{ini} is the average of the first 12 data points well before $\Delta t = 0$, and I_{sat} is the average of the last 12 data points, well after $\Delta t = 0$.

TABLE 2: Double Exponential Fit Coefficients of the $\chi^{*(2)}/\chi^{(2)}$ Ratio Showing the Fast and Slow Components

system	τ_1	τ_2
GeO ₂	163 ± 58 fs	3.7 ± 2.3 ps
GeS	< 100 fs	9.3 ± 4 ps
GeCl	< 100 fs	8.5 ± 4 ps

^a The $\chi^{*(2)}/\chi^{(2)}$ ratios were fitted to $A_0 + A_1 \exp(-t/\tau_1) + A_2 \exp(-t/\tau_2)$.

The physical origin of the evolution or phase of the $\chi^{*(2)}/\chi^{(2)}$ ratio cannot be determined directly by these experiments. However, on the basis of the time scales from the literature for electron thermalization in bulk Ge, suggestions can be made. The following fast and slow thermalization channels can be distinguished:

Fast: The excitation in Ge with 1.55-eV fundamental light will occur by direct absorption and creation of carriers around the Γ point. Following excitation in bulk Ge, the electrons dephase on the order of 10 fs.²⁷ Subsequently, the electrons scatter to the satellite X and L valleys on the order of 100 fs.²⁷ Because of the large density of states at X and L in Ge, Pauli blocking does not affect the electrons in Ge.²⁷ The light holes scatter to the heavy hole band in ~ 1 ps.²⁷

Slow: The electrons settle to the L valley, which is the global minimum in the conduction band, in ~ 4 ps.²⁷ Band gap renormalization (BGR) occurs in 1–4 ps. BGR is the shrinkage of the band gap due to exchange and correlation effects.²⁷ In 6 ps, the linear reflectivity recovers.²⁷ At the carrier density of these experiments ($\sim 3 \times 10^{19}$ cm⁻³), Auger recombination occurs in about 5.5 ns after excitation.

Although the time scales extracted for the evolution of Ge(111)–GeO₂ suggest that electron dynamics dominate the response and occur on a similar time scale as in the bulk, a similar conclusion does not appear to hold for Ge(111)–S and Ge(111)–Cl. The faster initial response, associated with intervalley electron scattering in the bulk, for Ge(111) surfaces terminated with heavier atoms suggests that these environments cause more rapid thermalization.

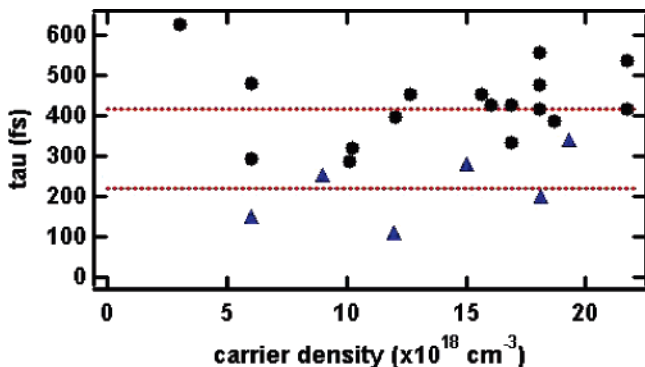


Figure 5. SHG response time constant (τ) vs carrier density. Average τ in the Ge(111)–GeO₂ system is 415 ± 90 fs, and in the Ge(111)–S system the average τ is 220 ± 85 fs; (●) Ge(111)–GeO₂, (▲) Ge(111)–S.

The lack of carrier-density dependence of the characteristic time scales of SHG, Figure 5, also suggests that electron–phonon, rather than carrier–carrier coupling, dominates the thermalization process. The lower phonon frequencies associated with heavier atoms result in a higher density of phonon states, possibly leading to greater coupling and rate of energy transfer from interfacial electrons to the interfacial phonon bath. Given the concerns regarding device degradation by hot-carrier thermalization at semiconductor–dielectric interfaces,¹⁶ the present results point to additional possible complications with the move to high k dielectrics employing heavy atoms.

Conclusions

The time-resolved SHG response of Ge(111)–GeO₂, Ge(111)–S, and Ge(111)–Cl depends markedly on the surface chemistry. The SHG signal increases at $t > 0$ for Ge(111)–GeO₂ but decreases for Ge(111)–S and Ge(111)–Cl. This phenomenon is attributed to the possibility that $\chi^{*(2)}$ might be in phase with $\chi^{(2)}$ for the Ge(111)–GeO₂ system but out of phase for the Ge(111)–S and Ge(111)–Cl systems. The ratio of the the hot carrier to the valence-band nonlinear susceptibilities was determined to be 924 ± 40 in the Ge(111)–GeO₂ system, -720 ± 50 in the Ge(111)–S system, and -880 ± 100 in the Ge(111)–Cl system. In the Ge(111)–GeO₂ system, the SHG response reaches a steady state in 415 ± 90 fs, in the Ge(111)–S system, 220 ± 85 fs, and in the Ge(111)–Cl system, 172 ± 50 fs.

Different chemical terminations clearly have a marked effect on the hot-carrier dynamics. The present results point to the importance of a proper choice of the alternative dielectric to be used in devices, as it will have a large effect on the carrier dynamics of the device, with consequences on device performance, degradation, and lifetime.

Acknowledgment. We acknowledge the generous support of the DOE, Office of Basic Energy Sciences.

References and Notes

- (1) Sze, S. M. *Physics of Semiconductor Devices*, 2nd ed.; Wiley: New York, 1981.
- (2) Wolkow, R. A. *Ann. Rev. Phys. Chem.* **1999**, *50*, 413–441.
- (3) Chui, C.; Kim, H.; Chi, D.; Triplett, B.; McIntyre, P.; Saraswat, K. *A Sub-400 Degree C Germanium MOSFET Technology with High -k Dielectric and Metal Gate*, International Electron Devices Meeting, San Francisco, CA, Dec 8–11, 2002.
- (4) Shang, H.; Okorn-Schmidt, H.; Chan, K.; Copel, M.; Ott, J.; Kozlowski, P.; Steen, S.; Cordes, S.; Wong, H.; Jones, E.; Haensch, W. *High Mobility p-Channel Germanium MOSFETs with a Thin Ge Oxynitride Gate Dielectric*, International Electron Devices Meeting, San Francisco, CA, Dec 8–11, 2002.
- (5) Balk, P. In *The Importance of the Si–SiO₂ System for Electronic Devices in the Si–SiO₂ System*; Balk, P., Ed.; Elsevier: Amsterdam, 1988; p 2–20.
- (6) Gusev, E. P. Ultrathin oxide films for advanced gate dielectrics applications. Current progress and future challenges. In *Defects in SiO₂ and Related Dielectrics: Science and Technology*; Pacchioni, L. S. G., Griscom, D. L., Eds.; Kluwer Academic Publishers: Boston, MA, 2000; p 557–579.
- (7) Buriak, J. M. *Chem. Commun.* **1999**, 1051–1060.
- (8) Pietsch, G. J. *Appl. Phys. A: Mater. Sci. Process.* **1995**, *60*, 347–363.
- (9) Bodlaki, D.; Yamamoto, H.; Waldeck, D. H.; Borguet, E. *Surf. Sci.* **2003**, *543*, 63–74.
- (10) Fomenko, V.; Bodlaki, D.; Faler, C.; Borguet, E. *J. Chem. Phys.* **2002**, *116*, 6745–6754.
- (11) Bansal, A.; Li, X.; Lauermann, I.; Lewis, N. S.; Yi, S. I.; Weinberg, W. H. *J. Am. Chem. Soc.* **1996**, *118*, 7225–7226.
- (12) Chabal, Y. J.; H. G. S.; Raghavachari, K.; Burrows, V. A. *J. Vac. Sci. Technol., A* **1989**, *7*, 2104–2109.
- (13) Higashi, G. S.; C. Y. J.; Trucks, G. W.; Raghavachari, K. *Appl. Phys. Lett.* **1990**, *56*, 656–658.
- (14) Linford, M. R.; Fenter, P.; Eisenberger, P. M.; Chidsey, C. E. D. *J. Am. Chem. Soc.* **1995**, *117*, 3145–3155.
- (15) Boukherroub, R.; Wayner, D. D. M. *J. Am. Chem. Soc.* **1999**, *121*, 11513–11515.
- (16) Hess, K.; Register, L. F.; McMahon, W.; Tuttle, B.; Aktas, O.; Ravaoli, U.; Lyding, J. W.; Kizilyalli, I. C. *Physica B* **1999**, *272*, 527–531.
- (17) Shen, Y. R. *Nature* **1989**, *337*, 519.
- (18) (a) Lüpke, G. *Surf. Sci. Rep.* **1999**, *35*, 75–161. (b) Downer, M. C.; Mendoza, B. S.; Garmenko, V. I. *Surf. Interf. Anal.* **2001**, *31*, 966–986.
- (19) Anderson, G. W.; Hanf, M. C.; Norton, P. R.; Lu, Z. H.; Graham, M. J. *Appl. Phys. Lett.* **1995**, *66*, 1123–1125.
- (20) Lyman, P. F.; Sakata, O.; Marasco, D. L.; Lee, T. L.; Breneman, K. D.; Keane, D. T.; Bedzyk, M. J. *Surf. Sci.* **2000**, *462*, L594–L598.
- (21) *CRC Handbook of Chemistry and Physics*, 79th ed.; Lide, D. R., Ed.; CRC Press: Boca Raton, FL, 1998; p 12–131.
- (22) Xu, J.; Almeida, R. *J. Sol–Gel Sci. Technol.* **2000**, *19*, 243–248.
- (23) Lu, Z. H. *Appl. Phys. Lett.* **1996**, *68*, 520–522.
- (24) Bodlaki, D.; Borguet, E. *Appl. Phys. Lett.* **2003**, *83*, 2357–2359.
- (25) McClelland, A.; Fomenko, V.; Borguet, E. *J. Phys. Chem. B* **2004**, *108*, 3789–3793.
- (26) Tanaka, T.; Harata, A.; Sawada, T. *J. Appl. Phys.* **1997**, *82*, 4033–4038.
- (27) Zollner, S.; Myers, K. D.; Jensen, K. G.; Dolan, J. M.; Bailey, D. W.; Stanton, C. J. *Solid State Commun.* **1997**, *104*, 51–55.